An Acad Bras Cienc (2024) 96(2): e20230126 DOI 10.1590/0001-3765202420230126
Anais da Academia Brasileira de Ciências | *Annals of the Brazilian Academy of Sciences*
Printed ISSN 0001-3765 I Online ISSN 1678-2690
www.scielo.br/aabc | www.fb.com/aabcjournal

GEOSCIENCES

Statistical modeling of maximum temperature in Guinea

MALICK KEBE & SARALEES NADARAJAH

Abstract: A statistical analysis of maximum temperature from twelve weather stations in parts of Guinea is provided. Using maximum likelihood estimation, maximum temperature data was fitted by the Generalized Extreme Value distribution. Data from all of the twelve stations were adequately fit by the Generalized Extreme Value distribution. Return level estimates are provided. Significant trends in maximum temperature were found for four of the stations. The four stations exhibited significant positive trends at the 5% significance level.

Key words: Generalized extreme value distribution, Estimation, Maximum likelihood, Return level

1 - INTRODUCTION

Guinea is a country on the west coast of Africa. It is bordered by Guinea-Bissao, Liberia, Sierra Leone, Senegal, Mali, Ivory Coast and the Atlantic ocean to the west. Figure 1 depicts Guinea along with its neighbors.

Guinea is home to a varied climate and copious biodiversity. It is separated into four natural geographical areas each with its own identifying geographic features. The four areas include coastal area (Lower / Coastal / Maritime Guinea), an area of plains (Middle Guinea), an area of Savannas (Upper Guinea), and an area of forests (Forested Guinea).

The Niger, Gambia, and Senegal rivers - west Africa's three most important rivers - are among the 22 west African rivers that originate in Guinea. Many more rivers originate from Guinea, earning it the name water tower of west Africa. Guinea is also the origin of four catchment basins. It's capital city which is an isthmus jutting out 36 kilometres into land with width varying from 0.2 to 6 kilometres and is one of the wettest cities in the world ($>$ 4000 millimetres of rain per year) with average temperature between 24 and 30 centigrade.

Guinea is a tropical country. It only has two seasons: rainy and dry seasons. While temperatures vary from one geographic area to another, Guinea is generally warm to hot.

In this paper, we focus on extreme land surface temperatures in Guinean weather stations. While rare, extreme temperatures are important to model because they can have disastrous effects on areas, infrastructure and people.

As temperatures rises above 35 centigrade, it is not as safe to be outside. In places like Guinea where agriculture is common and agriculture is an outside activity, high temperatures can be negative

Figure 1. Guinea and its bordering countries.

for health and can be dangerous for individuals. Furthermore, individuals whose profession entails remaining outdoors for extended periods of time (for example, construction workers) are at risk.

There is not much research or reports about accidents and deaths due to heat in Guinea, but they are bound to exist and may not be uncommon. Heat wave effects on individuals are scantly reported in Africa in general and Guinea in particular. Deaths due to complications associated with extreme heat are dubbed "silent killers" by some due to the fact that the impact is not readily seen with the naked eye like, for example, drowning from a flood (Smith et al. 2014). The factors which affect individuals are varied but are difficult to catalog (Stanke et al. 2013). As a consequence we are left with much missing data since no association is made between health issues and the high temperatures that caused them. In contrast, effects of temperature are well publicized in the western world.

We do not explore the effects of how increased temperatures affect individuals or how increased temperatures will affect Guinea's economy and health systems. There has been interesting research and results into the effects on extreme heat on Africa. We know however that extreme heat and rain disproportionally affect developing nations like Guinea.

High temperatures can lead to food insecurity too. Fundamental and ubiquitous staples like maize, millet, sorghum and wheat will be negatively impacted by rising temperatures as cereal crop productivity will be reduced as temperature increases. According to Pereira (2017), pressures from pests, weeds and diseases are also expected to increase with detrimental effects on crops. Increase in heat wave events will also lead to a loss of ability to keep livestock alive outdoors (Niang et al. 2014).

High temperatures may also lead to developmental problems. Tusting et al. (2020) tested the hypothesis that young children in Africa exposed to high temperatures will experience growth faltering. According to their analysis of data for children aged 0–5 years from 52 national surveys in sub-Saharan Africa, they discovered that monthly mean daytime land surface temperatures exceeding 35 centigrade were associated with a 27% increase in the odds of wasting, a 9% increase in the odds of underweight, a 23% increase in concurrent stunting with wasting, but a 10% reduction in stunting, compared with temperatures averaging less than 30 centigrade between 2000 and 2016.

Blom et al. (2022) discovered that extreme heat subjection increases the prevalence of both chronic and acute malnutrition in west Africa. This study involved children from 3 to 36 months from 1993 to 2014 and linked 15 rounds of repeated cross-section data from five west African countries to geo-coded weather data. Blom et al. (2022) found that growth stunting is increased by 7.4 percentage for a 2 centigrade rise in temperature. They remarked that the effect of temperature was threatening to undo efforts made over the years to improve child malnutrition in the region.

We are aware of only three papers studying effects of temperature in Guinea. Aguilar et al. (2009) examined changes in temperature extremes in western central Africa, Guinea Conakry, and Zimbabwe from 1955-2006. Loua et al. (2019) investigated inter-annual and annual changes in temperature by using monthly averaged temperature data without interruption of Conakry airport from 1960 to 2016. Loua et al. (2020) used a trend-run model to estimate the trend in surface temperatures recorded at twelve sites in Guinea from 1960 to 2016 and to examine the contribution of each climate forcing.

But none of these papers model extreme temperature in Guinea. This paper provides the first statistical modeling of extreme temperature in Guinea. We fit extreme value distributions to temperature data from twelve stations throughout the Republic of Guinea and seeks answers to the following questions and more: What are the hottest and coolest areas with respect to maximum temperature? What are the shapes of the distributions of maximum temperature? Does maximum temperature have an upper bound? What do the return curves look like for each region? Which region has the highest/lowest return curve? Is there any significant trend in maximum temperature from year to year?

The contents of the paper are organized as follows. Section 2 describes the data from twelve locations in Guinea: Boke, Conakry, Faranah Kankan, Kindia, Kissidougou, Koundara, Labe, Mamou, Macenta, Siguiri and Zerekore. These stations are diverse in climate and represent Guinea well as a whole. Section 3 describes the method used to analyze the data. Section 4 presents the results of the method and their discussion. The paper is concluded in Section 5.

2 - DATA

The data are monthly temperatures in centigrade for a period of at least 20 years for twelve stations: Boke, Conakry, Faranah Kankan, Kindia, Kissidougou, Koundara, Labe, Mamou, Macenta, Siguiri and Zerekore. The years of data are different for different stations: for Kindia, Boke, Kankan, Labe and Zerekore, the data are from 1991 to 2020; Koundara covers the years 1987-2019; Mamou covers the years 1990-2017; Faranah also covers years 1990-2017, but missing values for the years 2001, 2005, and 2012-2014; Siguiri covers the years 1982-2004, but missing values for the years 2001 and 2002; Kanakan covers the years 1990-2016; Kissidougou covers the years 1981-2009; Macenta covers the years 1940-2006. The data was obtained from the National Meteorology Service of Guinea.

The distribution of the data for each station was observed and errors resulting from data processing were not found. There were no anomalies or impossible values. Missing values were disregarded from the analysis.

For representativeness purposes, each of the four natural regions is home to three weather stations as follows: coastal Guinea region is home to Boke, Conakry, and Kindia stations; middle Guinea region is home of Koundara, Labe and Mamou; upper Guinea region is home to Faranah, Kankan and Siguiri stations; the forested region of Guinea includes Kissidougou, Macenta and Nzerekore stations. The twelve stations chosen correspond to stations where data are regularly collected and reliable (Kante et al. 2020).

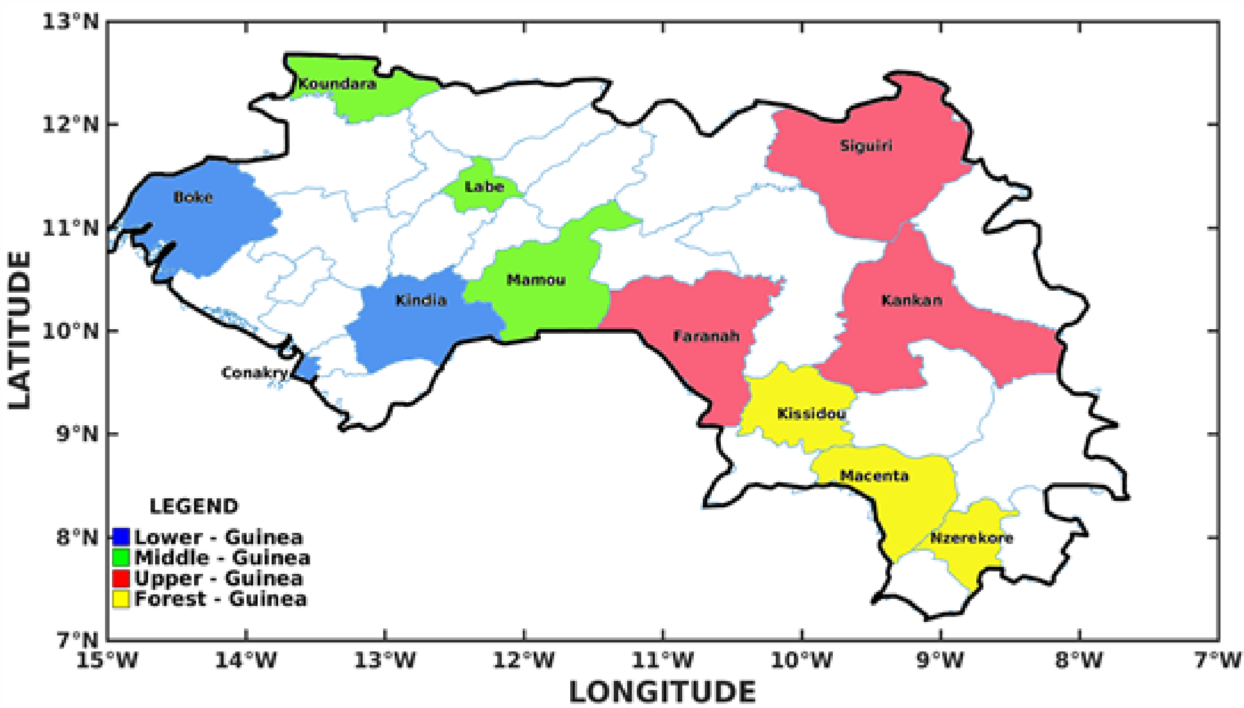

Figure 2. Geographic locations of the twelve stations (Kante et al. 2020).

Figure 2 shows the positions of the weather stations in Guinea. They are spread out over the nation and thus a good representation of the geography and meteorology. All of the different zones are accounted for. For example, each of the four geographic regions of Guinea is represented by three weather stations.

Typically, an event is called extreme if it lies above or below some pre-defined threshold. These thresholds are determined differently by different researchers leading to inconsistent meanings. In our case, the extreme is defined as the maximum numerical value of temperature collected by year and indicated by the weather stations. In the literature, some researchers investigate daily and even sub-daily extremes while others study extremes over a duration of days, weeks or months. We picked one-year interval due to interest in the maximal temperature per year of the data for each of the twelve weather stations.

We aggregated the data to get one single value for each year. Table I gives the number of years of record, mean, minimum, maximum, median, standard deviation, coefficient of variation, skewness and kurtosis.

Table I. The mean, minimum, maximum, median, standard deviation, coefficient of variation, skewness and the kurtosis of the maximum temperature values.

Station	Count	Mean	Minimum	Maximum	Median	Standard deviation	Coefficient of variation	Skewness	Kurtosis
Kankan	27	37.952	36.4	39.3	38	0.694	0.018	-0.514	3.172
Kindia	30	35.943	34.9	37.0	35.90	0.470	0.013	0.106	3.068
Faranah	23	36.643	33.4	39.1	36.90	1.262	0.034	-0.913	4.423
Boke	30	38.043	36.0	39.2	38.20	0.840	0.022	-0.551	2.457
Conakry	30	32.490	31.1	33.9	32.55	0.659	0.020	-0.052	2.446
Koundara	33	40.448	37.6	41.8	40.60	0.810	0.020	-1.351	5.951
Kissidougou	29	34.624	33.6	36.0	34.70	0.600	0.017	0.308	2.515
Labe	31	33.748	32.3	35.4	33.70	0.672	0.020	0.367	3.205
Macenta	63	33.030	30.8	35.2	33.10	1.080	0.033	-0.260	2.485
Mamou	24	34.367	33.3	34.5	34.45	0.587	0.017	-0.077	2.418
Siguiri	21	38.476	35.5	40.3	38.60	1.091	0.028	-0.819	4.026
Zerekore	28	33.336	32.0	35.2	33.20	0.806	0.024	0.863	3.226

The mean maximum temperature is smallest for Conakry and largest for Koundara. The minimum of the maximum temperature is smallest for Macenta and largest for Koundara. The maximum of the maximum temperature is smallest for Conakry and largest for Koundara. The median maximum temperature is smallest for Conakry and largest for Koundara. The standard deviation of the maximum temperature is smallest for Kindia and largest for Faranah. The coefficient of variation of the maximum temperature is smallest for Kindia and largest for Faranah.

The skewness is positive for Kindia, Kissidougou, Labe and Zerekore. The skewness is negative for the remaining stations. The largest of the positive skewness is for Zerekore. The smallest is for Kindia. The largest of the negative skewness is for Faranah. The smallest is for Conakry.

The kurtosis values for Kankan, Kindia, Faranah, Koundara, Labe, Siguiri and Zerekore are greater than 3 (not by much for Kankan and Kindia). Graphically, their distributions are more peaked and have fatter tails than the normal distribution. They are leptokurtic. The stations at Boke, Conakory, Kissidougou, Macenta and Mamou have kurtosis values less than 3. Graphically, they are less peaked and more pinched tails than the normal distribution. They are platykurtic. The kurtosis is smallest for Mamou and largest for Koundara.

3 - METHODS

Let X denote a random variable representing the monthly maximum temperature. According to extreme value theory (see Leadbetter et al. (1983), Resnick (1987) and Embrechts et al. (1997)), the cumulative distribution function of X can be approximated by

$$F_X(x) = \exp\left[-\left(1+\xi\frac{x-\mu}{\sigma}\right)^{-1/\xi}\right] \tag{1}$$

for $\mu-\sigma/\xi \leq x < \infty$ if $\xi > 0$, $-\infty < x < \infty$ if $\xi = 0$ and $-\infty < x \leq \mu-\sigma/\xi$ if $\xi < 0$, where $-\infty < \mu < \infty$ denotes a location parameter, $\sigma > 0$ denotes a scale parameter and $-\infty < \xi < \infty$ denotes a shape parameter. Note that if $\xi > 0$ then X has a heavy tail bounded below by $\mu - \sigma/\xi$. If $\xi < 0$ then X has a short tail bounded above by $\mu - \sigma/\xi$.

The distribution in (1) is known as the Generalized Extreme Value (GEV) distribution. The GEV distribution was fitted to the data in Section 2 by the method of maximum likelihood. Suppose $x_1, x_2, \ldots, x_n$ is an enumeration of the data in Section 2. The maximum likelihood estimates of μ, σ and ξ were obtained by maximizing

$$L(\mu,\sigma,\xi) = \frac{1}{\sigma^n}\prod_{i=1}^{n}\left\{\left(1+\xi\frac{x_i-\mu}{\sigma}\right)^{-\frac{1}{\xi}-1}\exp\left[-\left(1+\xi\frac{x_i-\mu}{\sigma}\right)^{-\frac{1}{\xi}}\right]\right\} \tag{2}$$

over all possible values of μ, σ and ξ. The maximum likelihood estimates are the values of μ, σ and ξ corresponding to the maximum of $L(\mu,\sigma,\xi)$. The maximization was performed using the command fgev in the R package evd (Stephenson 2018, R Core Team 2022). Other distributions (for example, the normal distribution) may provide better fits to the monthly maximum temperature. But the GEV distribution is theoretically justified.

Let $\widehat{\mu}$, $\widehat{\sigma}$ and $\widehat{\xi}$ denote the maximum likelihood estimates of μ, σ and ξ, respectively. A quantity of interest based on (1) is the T-year return level loosely interpreted as the monthly maximum temperature expected on average once in every T years. Let x_T denote the T-year return level corresponding to (1). It must satisfy

$$F_X\left(x_T\right) = 1-\frac{1}{T}. \tag{3}$$

Inverting (3), we obtain

$$x_T = \widehat{\mu} + \frac{\widehat{\sigma}}{\widehat{\xi}}\left\{\left[-\log\left(1-\frac{1}{T}\right)\right]^{-\widehat{\xi}} - 1\right\}. \tag{4}$$

See equation (3.4) in Coles (2001).

4 - RESULTS AND DISCUSSION

The GEV distribution was fitted to monthly maximum temperature data from all twelve weather stations. Table II shows the estimates, standard errors, and 95% confidence intervals for the GEV parameters.

Table II. Parameter estimates, standard errors and confidence intervals for the fitted GEV distribution.

		μ	σ	ξ
Kankan	Parameter estimates	37.751	0.725	-0.404
	Standard errors	0.151	0.107	0.107
	Confidence interval (95%)	(37.454, 38.048)	(0.516, 0.935)	(-0.612, -0.195)
Kindia	Parameter estimates	35.774	0.456	-0.252
	Standard errors	0.092	0.063	0.110
	Confidence interval (95%)	(35.595, 35.954)	(0.333,0.580)	(-0.468,-0.036)
Faranah	Parameter estimates	36.289	1.339	-0.419
	Standard errors	0.301	0.206	0.100
	Confidence interval (95%)	(35.700, 36.878)	(0.936, 1.742)	(-0.616, -0.222)
Boke	Parameter estimates	37.940	0.948	-0.735
	Standard errors	0.187	0.171	0.152
	Confidence interval (95%)	(37.573, 38.307)	(0.613, 1.284)	(-1.033, -0.437)
Conakry	Parameter estimates	32.269	0.654	-0.309
	Standard errors	0.132	0.094	0.118
	Confidence interval (95%)	(32.011, 32.527)	(0.469, 0.838)	(-0.540, -0.077)
Koundara	Parameter estimates	40.267	0.864	-0.532
	Standard errors	0.161	0.117	0.089
	Confidence interval (95%)	(39.952, 40.583)	(0.634, 1.094)	(-0.707, -0.356)
Kissidougou	Parameter estimates	34.390	0.545	-0.181
	Standard errors	0.115	0.083	0.150
	Confidence interval (95%)	(34.164, 34.616)	(0.382, 0.708)	(-0.475, 0.113)
Labe	Parameter estimates	33.490	0.622	-0.188
	Standard errors	0.123	0.085	0.110
	Confidence interval (95%)	(33.249, 33.731)	(0.456, 0.788)	(-0.403, 0.028)
Macenta	Parameter estimates	32.705	1.121	-0.386
	Standard errors	0.155	0.112	0.081
	Confidence interval (95%)	(32.402,33.009)	(0.901, 1.341)	(-0.544, -0.228)
Mamou	Parameter estimates	34.179	0.586	-0.337
	Standard errors	0.133	0.097	0.148
	Confidence interval (95%)	(33.918, 34.440)	(0.397, 0.775)	(-0.627, -0.047)
Siguiri	Parameter estimates	38.217	1.157	-0.500
	Standard errors	0.273	0.202	0.133
	Confidence interval (95%)	(37.681, 38.753)	(0.760, 1.554)	(-0.761, 0.240)
Zerekore	Parameter estimates	32.974	0.617	0.005
	Standard errors	0.132	0.096	0.145
	Confidence interval (95%)	(32.716,33.232)	(0.429, 0.804)	(-0.279, 0.288)

Kankan, Kindia, Faranah, Boke, Conakry, Koundara, Macenta and Mamou have shape parameter estimates significantly negative. The smallest of these estimates is for Boke and the largest is for Kindia. For these eight stations, the maximum temperature is bounded above by $\widehat{\mu} - \widehat{\sigma}/\widehat{\xi}$, referred to as the probable maximum temperature. The estimates of the probable maximum temperature are 39.545, 37.584, 39.485, 39.230, 34.386, 41.891, 35.609 and 35.920 for Kankan, Kindia, Faranah, Boke, Conakry, Koundara, Macenta, and Mamou, respectively. The probable maximum temperature is largest for Koundara and smallest for Conakry.

Kissidougou, Labe, Siguiri and Zerekore have shape parameter estimates not significantly different from zero since zero is included in the 95% confidence intervals. The standard error of the shape parameter estimates is smallest for Macenta and largest for Boke.

The location parameter estimate is smallest for Conakry and largest for Koundara. Its standard error is smallest for Kindia and largest for Faranah. The scale parameter estimate is smallest for Kindia and largest for Faranah. Its standard error is also smallest for Kindia and largest for Faranah.

Probability and quantile plots are used to check the fit of the GEV distribution for each station. These plots for the twelve stations are shown in Figures 3 and 4.

Let $x_{(1)} \leq x_{(2)} \leq \cdots \leq x_{(n)}$ denote the data $x_1, x_2, \ldots, x_n$ arranged in increasing order. Let

$$\widehat{F}(x) = \exp\left[-\left(1 + \widehat{\xi}\frac{x - \widehat{\mu}}{\widehat{\sigma}}\right)^{-\frac{1}{\widehat{\xi}}}\right].$$

denote the fitted cumulative distribution function of the GEV distribution. Furthermore, let $\widehat{F}^{-1}(\cdot)$ denote the inverse function of $\widehat{F}(\cdot)$. Plots of $\widehat{F}\left(x_{(i)}\right)$, the observed probabilities, versus $i/(n+1)$, the expected probabilities, are known as probability plots. The observed and expected probabilities being equal corresponds to the diagonal straight lines in Figure 3. The 95% simulated confidence intervals of the observed probabilities are the dashed lines in Figure 3. Plots of $x_{(i)}$, the observed quantiles, versus $\widehat{F}^{-1}(i/(n+1))$, the expected quantiles, are known as quantile plots. The observed and expected quantiles being equal corresponds to the diagonal straight lines in Figure 4. The 95% simulated confidence intervals of the expected quantiles are the dashed lines in Figure 4. For the fit of the GEV distribution to be considered adequate, the plotted points in Figures 3 and 4 must be as close as possible to the diagonal lines and they must lie within the simulated confidence intervals. Figures 3 and 4 show clearly that the fits for the twelve locations are adequate.

In addition to using probability and quantile plots, we tested goodness of fit using the Kolmogorov-Smirnov, Anderson-Darling and Cramer-von Mises tests. The Kolmogorov-Smirnov test gave the p-values of 0.396, 0.959, 0.116, 0.612, 0.707, 0.724, 0.789, 0.906, 0.836, 0.267, 0.246 and 0.403 for the twelve locations. The Anderson-Darling test gave the p-values of 0.653, 0.469, 0.729, 0.967, 0.665, 0.540, 0.853, 0.643, 0.621, 0.099, 0.249 and 0.984. The Cramer-von Mises test gave the p-values of 0.607, 0.759, 0.632, 0.583, 0.876, 0.572, 0.690, 0.602, 0.117, 0.575, 0.322 and 0.732.

The return curves tell us how the temperature extremes might change in the future. While a return curve does not tell us when these temperatures will be reached, it does tell us how often we can expect, on average certain events in a given period of time. It also tells us how severe those events can be. This gives us a tool for preparation and putting policies into place.

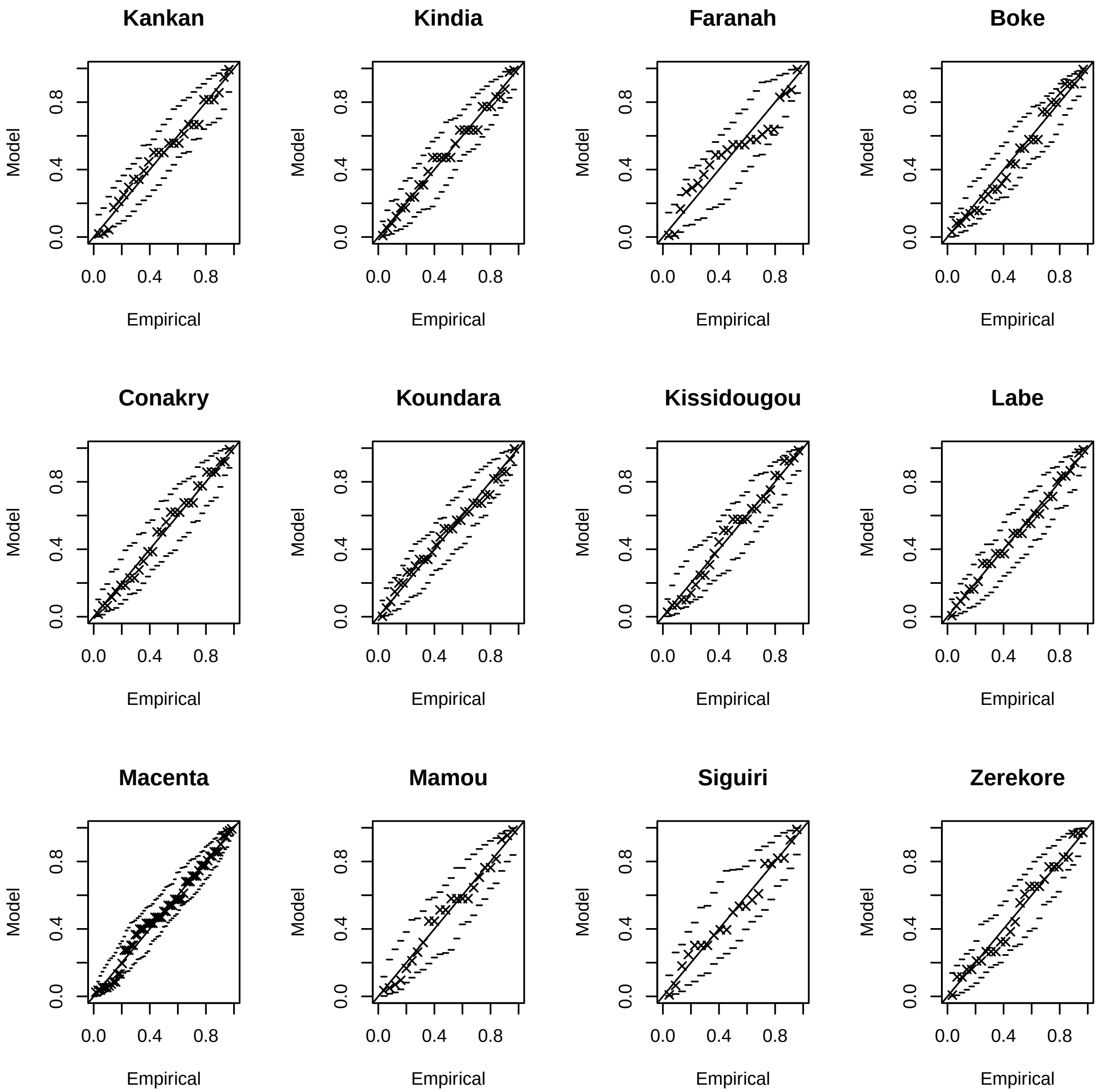

Figure 3. Observed probabilities against expected probabilities for the fit of the GEV distribution.

A higher return curve signals that we can expect higher temperatures on average over a fixed period of time than a lower return curve. Stations with higher return curves are more likely to experience extreme temperatures based on historical data.

We can interpret the return level as the value expected to be surpassed on average once every $T = 1/p$, where $1 - p$ is the probability associated with the quantile. x_{100} can be interpreted as the temperature we might expect to be exceeded once in a hundred years (this could be used to inform heat mitigation, for example). Although we use "return level", it is important to emphasize that a 100 year temperature event - a hot event with a 1% change of occurring in any given year - could materialize once, twice or more, or none at all in a 100 year interval.

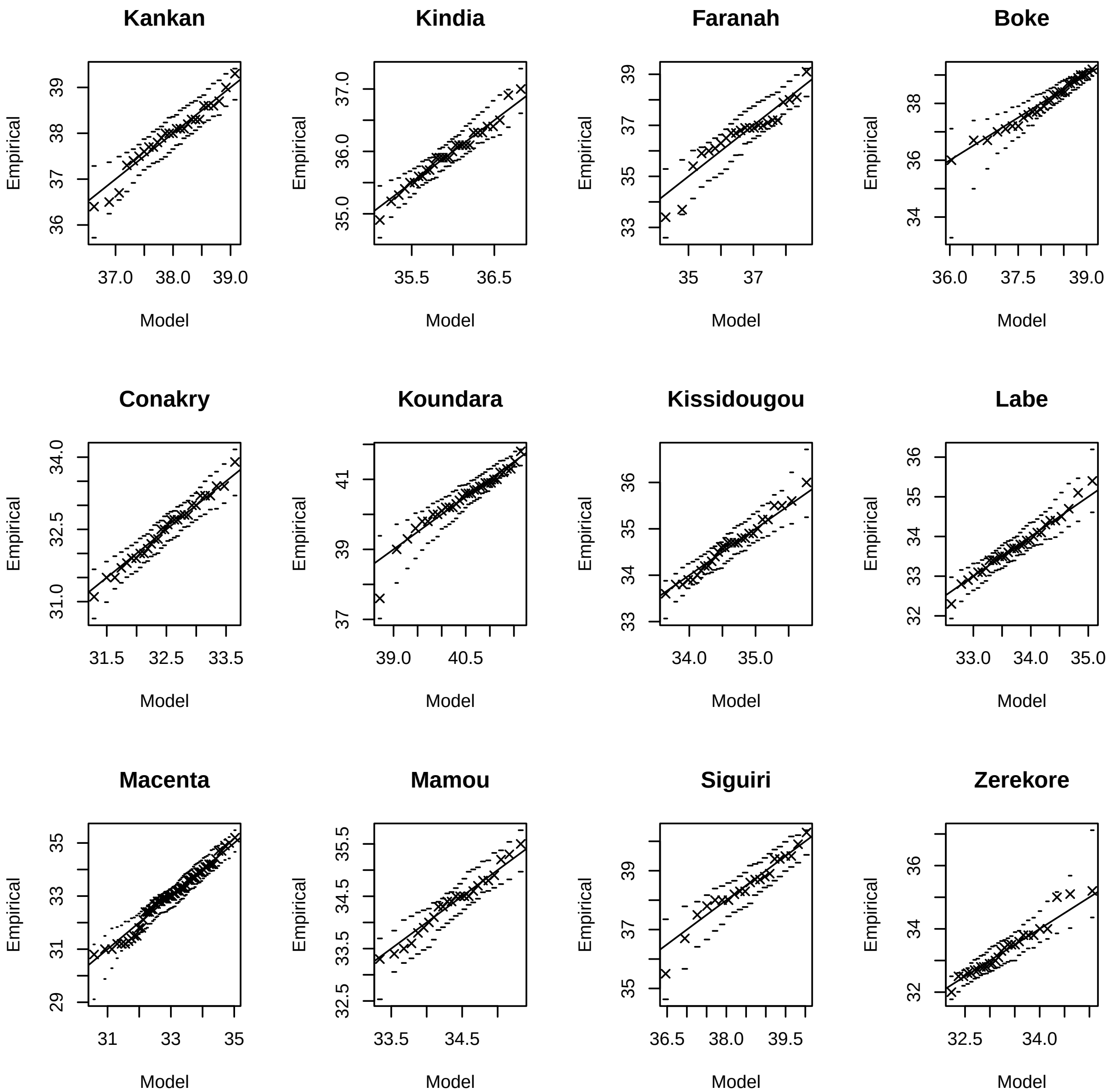

Figure 4. Observed quantiles against expected probabilities for the fit of the GEV distribution.

Plots of x_T for $T = 2, \ldots, 100$ are shown in Figure 5 and Figures S1, S2, S3 for the four natural geographical areas. Figure S4 shows all twelve return plots juxtaposed against each other. The return level estimates are highest for Koundara and Siguiri with Kankan and Boke approximately equal. They are lowest for Conakry, Macenta and Labe.

For coastal Guinea, the order of return curve height is Boke, Kindia and Conakry. Indeed, Boke is generally the hottest of the three locations. While Conakry is historically a rainy city, its temperature is uniformly hot but not as warm as Boke and Kindia. Boke is, on average, the hottest city in Guinea. The curves show that in terms of 100 year events, Boke is most likely to return more extreme temperatures.

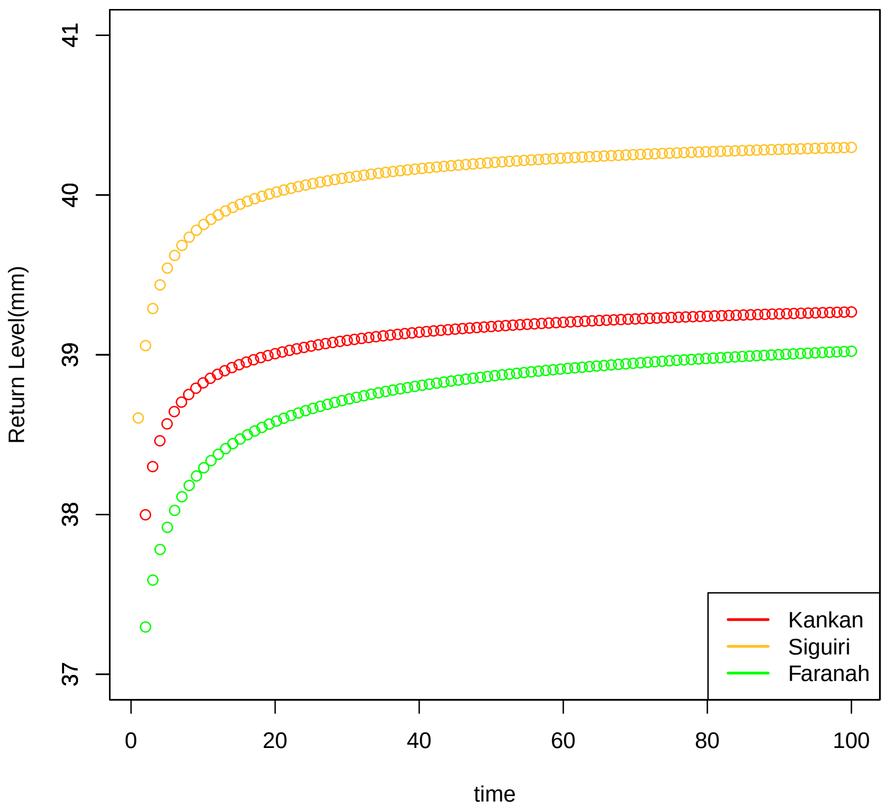

Figure 5. Estimates of x_T versus $T = 2, 3, \ldots, 100$ for upper Guinea.

Temperatures are lower/higher in middle Guinea than on the coastal Guinea. It seems that as if there is an inverse relationship between altitude and height of return curves. Labe has the highest altitude yet the lowest return curve. Mamou is between Labe and Koundara in terms of altitude as well as return curve height. Koundara is the least elevated of the three cities but has the highest return curve. In middle Guinea, height seems to be playing a negative tempering effect.

Upper Guinea has longer summer periods than other regions. It can be very hot in the daytime but temperatures tend to cool down in the evenings. Siguiri has the highest return curve in this region overall. Kankan and Faranah's curves are noticeably lower than Siguiri's, but close to each other. The return curves seem to confirm upper Guinea's notoriously drier, desert-like climate.

Forested Guinea has a somewhat wide variation relative to the other regions. Macenta's return curve is second lowest to Conakry while Zerekore and Kissidougou come around the middle of the pack. Zerekore was historically humid, but it has been warming up over the years. This could be related to climate change with links to deforestation (Loua et al. 2017).

Lastly, we investigated the presence or absence of a trend in stations' maximal recorded temperatures. We thus fitted (1) with the location parameter $\mu = a + b \times$ (Year-Initial Year), where a is the intercept parameter and b is the trend parameter. We can decide whether the trend is significant by comparing the largest value of

$$L(\mu,\sigma,a,b)=\frac{1}{\sigma^n}\prod_{i=1}^{n}\left\{\left(1+\xi\frac{x_i-a-b\times(\text{Year-Initial Year})}{\sigma}\right)^{-\frac{1}{\xi}-1}\right.$$
$$\left.\cdot\exp\left[-\left(1+\xi\frac{x_i-a-b\times(\text{Year-Initial Year})}{\sigma}\right)^{-\frac{1}{\xi}}\right]\right\}$$

with that of (2). If twice the difference of the logarithms of the likelihoods is greater than 3.841 then we can reject the null hypothesis assuming no trend at the 5% level of significance.

We found that there was some trend present. Specifically, there were significant positive linear trends at the Kankan, Kindia, Faranah, and Labe stations. Estimates of a and b, their standard errors, and p-values signifying the significance of the trends are given in Table III. Note that both Faranah and Kankan are in upper Guinea. Both Labe and Kindia are in middle Guinea. None of the stations exhibiting trends are in coastal Guinea or the forested region of Guinea. None of the stations exhibited significant negative linear trends.

Table III. Stations exhibiting significant linear trends in the μ parameter.

Station	Trend	$\hat{a}$ (se)	$\hat{b}$ (se)	p-value
Kindia	Positive	35.265 (0.132)	0.351 (0.008)	0.004
Faranah	Positive	35.383 (0.320)	0.094 (0.01)	0.000
Labe	Positive	32.896 (0.210)	0.041 (0.011)	0.003
Kankan	Positive	37.269 (0.189)	0.039 (0.009)	0.001

One explanation for these trends is urbanization. Urbanization – the concentration of populations into areas – can lead to increase of maximal temperatures through heat islands (as compared to outlying areas) caused by human activities. While all the stations are located in urban areas, Kankan, Kindia, Labe, Faranah and Kindia are among the most populated (World Bank 2018). Census data from 1996 to 2014 shows considerable increase in population during those years (Guinea 2015). The concentration of individuals ushers a demand for the land transformation in order to satisfy transportational (through the opening of roads), commercial, residential (building homes, energy, etc) and other uses.

Deforestation - another explanation for the trends - is devastating for the environment and leads to increasing maximal temperatures. Among the reported reasons for deforestation are increased space to graze livestock, palm oil production, woodfuel and/or charcoal needs. In terms of oil palm production in Guinea, Zerekore is first with 71%. Faranah is far behind with 12% of total palm oil production and Kindia is third with 10% of total palm oil production (USDA 2020). While most of the palm oil percentage comes from Zerekore, we should recall that Zerekore is a highly forested with more capacity to withstand deforestation than either Kindia or Faranah.

Deforestation is unfortunate because felled trees released stored CO2 gas back into the atmosphere. Studies have shown that deforestation does cause temperatures to rise and could indeed contribute to rising temperatures (Bright et al. 2017). Some people fell trees to clear out more space for agriculture. Ironically, these actions lead to detrimental degradation of both forest and soils making agriculture ineffective. As relating to the four stations displaying trends, they (along with two other stations) were targeted in 2019 as cities where reforestration could produce some benefits (Guinea 2020). Indeed in 2019, 31, 34, 39, and 13 trees were planted at Kankan, Kindia, Faranah, and Labe, respectively. Boke (26) the hottest city in Guinea, and Zerekore (36) an important city in forested Guinea are the other sites which were deemed important for planting of trees.

Chen and Dirmeyer (2020) found that, spatially, stronger land surface temperature sensitivity is found over arid or semi-arid regions such as in African savanna regions. Kankan and Faranah are located in upper Guinea, a natural region characterized by its savannas and therefore could be more temperature sensitive to deforestation efforts.

Note from (1) that $F_X(\mu) = \exp(-1) \approx 0.368$. Hence, the 36.8th percentile of the maximum temperature at Kindia increases by 0.351 centigrade per year, the 36.8th percentile of the maximum temperature at Faranah increases by 0.094 centigrade per year, the 36.8th percentile of the maximum temperature at Labe increases by 0.41 centigrade per year, and the 36.8th percentile of the maximum temperature at Kankan increases by 0.039 centigrade per year. The sharpest of the increases is for Kindia and the least sharpest of the increases is for Kankan. Furthermore, the 36.8th percentile of the maximum temperature at Kindia in 1991 ss 35.265 centigrade, the 36.8th percentile of the maximum temperature at Faranah in 1990 is 35.383 centigrade per year, the 36.8th percentile of the maximum temperature at Labe in 1991 is 32.896 centigrade per year, and the 36.8th percentile of the maximum temperature at Kankan in 1990 is 37.269 centigrade per year. The standard errors are reasonably small compared to the parameter estimates especially for the intercept parameter.

With our limited data, we do not possess sufficient granularity in order to notice a significant effect. Our findings contradict with Loua et al. (2019). According to Loua et al. (2019), temperature increased significantly at all but the Macenta station. However, Loua et al. (2019) analyzed temperature time series consisting of monthly averages from the 1960–2016 period.

It would be useful to develop early warning systems to alert people as to when temperatures could be very hot. A collaboration and synergy between weather and media services (television, radio, text messages) as well as local leaders (as canvassers or community meeting organizers) could help to reach more people than would otherwise be possible. Authorities could require that construction workers not work during the hottest part of the days or whenever there are extreme heat waves. Awareness raising campaigns to explain the deleterious effects of extreme heat on the body can also act as effective early warning systems.

It is also recommended to set up cooling centers as they may serve as places to keep the elderly, other vulnerable individuals, farmers and construction workers cool and help them avoid overheating and the consequences associated with extreme heat. However, some parts of Guinea may not be able to afford the energy generation requisites to employ cooling centers. In that case, it might be possible to invoke the equity principle from the Paris agreement and request subsidies from bigger polluters to offset some of negative externalities for which they are responsible for. It is highly recommended that these cooling centers release minimal carbon into the atmosphere.

Another recommendation is to take advantage of the carbon sinking property of trees. Reforestration efforts will be important to undertake. Planting trees - in new as well as old areas -

can contribute to mitigate increasing temperatures since forests and trees help to sequestrate carbon dioxide. The creation of green spaces like parks is known to reduce temperatures (Fallmann et al. 2013). Deployment of such practices could be useful in all areas but especially areas exhibiting positive trends such as Faranah, Kankan, Kindia, and Labe.

Cool roofs may go some distance in reducing ambient temperatures. A cool roof functions by efficiently reflecting light off its surface as well as emitting away heat that was absorbed. Cool roofs are more efficient than regular roofs and can sometimes be accomplished by simply applying a special coat on the regular roof. Using cool roofs and cool walls in homes, schools, and buildings is likely to make a difference in ambient temperatures because they limit the amount of heat piloted into dwellings and other buildings. It is entirely possible that jobs could be created from such endeavors.

The two previous ideas can be combined to make green roofs - roofs which are partially or completely covered with vegetation. According to Gilabert et al. (2021), this has a dual advantage of reducing temperatures through a phenomenon known as evapotranspiration and reducing carbon dioxide via photosynthesis.

Finally, policy makers can also look at crop intensification. By getting more yield, for an equal amount of land, forests will less likely to be destroyed. Trees can remain allies, and an ever growing population can continue to be fed without negative consequences for the environment.

5 - CONCLUSIONS

This paper has provided the first extreme value statistical analysis of maximum temperature using data from twelve weather stations peppered across Guinea. As assessed by probability plots, quantile plots Kolmogorov-Smirnov tests, Anderson-Darling tests and Cramer-von Mises tests, the generalized extreme value distribution allowed for an adequate fit to the data from all stations. Using historical data, we generated return curves. The hottest stations in terms of extreme heat are Koundara and Siguiri with Kankan and Boke approximately equal. The least hot stations in terms of extreme heat are Conakry, Macenta, and Labe.

Four of the stations exhibited significant positive trends at the 5% significance level. They are Kankan, Kindia, Faranah and Labe. None of the stations exhibited significant negative trends. Hence, Faranah, Kankan, Kindia, and Labe are most affected by climate (even though with the exception of Kankan, they are not among the hottest in terms of mean temperature).

Although we were looking at many years worth of data, because we aggregated at the yearly level, the data is coarse grained. It would be interesting to see daily data in order to make statements about the prevalence of heat waves and their frequency of occurrence over time. The sustained nature of heatwaves is much more likely to lead to negative consequences than a rare, one off occurrence. Weekly extreme temperature data would not be as useful as, say, monthly extreme temperature data.

Future directions in terms of modeling could include an analysis of extreme temperature by the generalized Pareto distribution, looking at how coldest temperatures relate to warmest temperatures, and analysis of the relationship between extreme precipitation and extreme high or low temperatures.

Acknowledgments

Both authors are grateful to the Guinean Meteorological Service (GMS) for providing the temperature data.

REFERENCES

AGUILAR E ET AL. 2009. Changes in temperature and precipitation extremes in western central Africa, Guinea Conakry, and Zimbabwe, 1955-2006. J Geophys Res Atmos 114, article number D02115.

BLOM S, ORTIZ-BOBEA A & HODDINOTT J. 2022. Heat exposure and child nutrition: Evidence from west Africa. J Environ Econ Manag 115, article number 102698.

BRIGHT RM, DAVIN E, O'HALLORAN T, PONGRATZ J, ZHAO K & CESCATTI A. 2017. Local temperature response to land cover and management change driven by non-radiative processes. Nat Clim Change 7: 296-302.

CHEN L & DIRMEYER P A. 2020. Reconciling the disagreement between observed and simulated temperature responses to deforestation. Nat Commun 11: 1-10.

COLES SG. 2001. An introduction to statistical modeling of extreme values. New York: Springer Verlag.

EMBRECHTS P, KLÜPPELBERG C & MIKOSCH T. 1997. Modelling extremal events for insurance and finance. Berlin: Springer Verlag.

FALLMANN J, EMEIS S & SUPPAN P. 2013. Mitigation of urban heat stress–a modelling case study for the area of Stuttgart. DIE ERDE–Journal of the Geographical Society of Berlin 144: 202-216.

GILABERT J, VENTURA S, SEGURA R, MARTILLI A, BADIA A, LLASAT C, CORBERA J & VILLALBA G. 2021. Abating heat waves in a coastal Mediterranean city: What can cool roofs and vegetation contribute? Urban Clim 37, article number 100863.

GUINEA. 2015. Institut national de la statistique, Guinea. https://web.archive.org/web/20151124030052/http://www.geohive.com/cntry/guinea.aspx.

GUINEA. 2020. Annuaire des statistiques forestieres 2018-2019. Ministere de l'environnement des eaux et forets, URL https://www.stat-guinee.org/images/Documents/Publications/SSN/meef/Annuaire_statistique_forestiere_2018\%20-2019.pdf.

KANTE IK, SALL SM, BADIANE D, DIOUF I, DIENG AL, DIABY I & GUICHARD F. 2020. Analysis of rainfall dynamics in Conakry, Republic of Guinea. Atmospheric and Climate Sciences 10: 1-20.

LEADBETTER MR, LINDGREN G & ROOTZÉN H. 1983. Extremes and related properties of random sequences and processes. New York: Springer Verlag.

LOUA RT, BEAVOGUI M, BENCHERIF H, BAMBA Z & AMORY-MAZAUDIER C. 2017. Climatology of Guinea: Study of climate variability in N'zerekore. Journal of Agricultural Science and Technology A 7, doi: 10.17265/2161-6256/2017.04.001.

LOUA RT, BENCHERIF H, BEGUE N, MBATHA N, PORTAFAIX T, HAUCHECORNE A, SIVAKUMAR V & BAMBA Z. 2020. Surface temperature trend estimation over 12 sites in Guinea using 57 years of ground-based data. Climate 8, article number 68.

LOUA R T, BENCHERIF H, MBATHA N, BEGUE N, HAUCHECORNE A, BAMBA Z & SIVAKUMAR V. 2019. Study on temporal variations of surface temperature and rainfall at Conakry airport, Guinea: 1960-2016. Climate 7, article number 93.

NIANG I, RUPPEL OC, ABDRABO MA, ESSEL A, LENNARD C, PADGHAM J & URQUHART P. 2014. Africa. In: Climate Change 2014 – Impacts, Adaptation, and Vulnerability, Part B – Regional Aspects (editors V. R. Barros, C. B. Field, D. J. Dokken, M. D. Mastrandrea, K. J. Mach, T. E. Bilir, M. Chatterjee, K. L. Ebi, Y. O. Estrada, R. C. Genova, B. Girma, E. S. Kissel, A. N. Levy, S. MacCracken, P. R. Mastrandrea and L. L. White), Contribution of Working Group II to the Fifth Assessment Report of the Intergovernmental Panel on Climate Change, Cambridge: Cambridge University Press, pp. 1199-1265.

PEREIRA L. 2017. Climate change impacts on agriculture across Africa. Oxford Research Encyclopedia of Environmental Science.

R CORE TEAM. 2022. R: A language and environment for statistical computing. Vienna, Austria: R Foundation for Statistical Computing.

RESNICK SI. 1987. Extreme values, regular variation and point processes. New York: Springer Verlag.

SMITH KR ET AL. 2014. Human health: Impacts, adaptation, and co-benefits. In: Climate Change 2014 – Impacts, Adaptation, and Vulnerability, Part A – Global and Sectoral Aspects – Working Group II Contribution to the Fifth Assessment Report of the Intergovernmental Panel on Climate Change, Cambridge: Cambridge University Press, p. 709-754.

STANKE C, KERAC M, PRUDHOMME C, MEDLOCK J & MURRAY V. 2013. Health effects of drought: A systematic review of the evidence. PloS Currents 1, doi: 10.1371/currents.dis.7a2cee9e980f91ad7697b570bcc4b004.

STEPHENSON A. 2018. evd: Functions for extreme value distributions. R package version 2.3-3.

TUSTING LS, BRADLEY J, BHATT S, GIBSON HS, WEISS DJ, SHENTON FC & LINDSAY SW. 2020. Environmental temperature and growth faltering in African children: A cross-sectional study. The Lancet Planetary Health 4: e116-e123.

USDA. 2020. Foreign agricultural service palm oil production 2020 long rains (Mar - Dec). URL https://ipad.fas.usda.gov/cropexplorer/cropview/comm_chartview.aspx?fattributeid=1&cropid=4243000&startrow=21&sel_year=2020&ftypeid=60&regionid=wafrica&cntryid=GIN&nationalGraph=False.

WORLD BANK. 2018. The challenges of urbanization in West Africa. Washington, DC: AFCW3 Economic Update.

SUPPLEMENTARY MATERIAL

Figures S1, S2, S3, S4.

How to cite
KEBE M & NADARAJAH S. 2024. Statistical modeling of maximum temperature in Guinea. An Acad Bras Cienc 96: e20230126. DOI 10.1590/0001-3765202420230126.

Manuscript received on February 8, 2023;
accepted for publication on February 19, 2024

MALICK KEBE[1]
https://orcid.org/0009-0008-3098-1168

SARALEES NADARAJAH[2]
https://orcid.org/0000-0002-7505-7066

[1]Department of Mathematics, Howard University, Washington DC 20051, USA
[2]Department of Mathematics, University of Manchester, Manchester M13 9PL, UK

Correspondence to: **Saralees Nadarajah**

E-mail: Saralees.Nadarajah@manchester.ac.uk

Author contributions

Both authors contributed equally to the manuscript.